

## Timing calibration and directional reconstruction for Tunka-HiSCORE

This content has been downloaded from IOPscience. Please scroll down to see the full text.

2015 J. Phys.: Conf. Ser. 632 012041

(<http://iopscience.iop.org/1742-6596/632/1/012041>)

View [the table of contents for this issue](#), or go to the [journal homepage](#) for more

Download details:

IP Address: 141.34.3.98

This content was downloaded on 26/01/2016 at 09:56

Please note that [terms and conditions apply](#).

# Timing calibration and directional reconstruction for Tunka-HiSCORE

A.Porelli<sup>2</sup>, D.Bogorodskii<sup>5</sup>, M.Brückner<sup>6</sup>, N.Budnev<sup>5</sup>, O.Chvalaev<sup>5</sup>,  
A.Dyachok<sup>5</sup>, S.Epimakhov<sup>1</sup>, T.Eremin<sup>3</sup>, O.Gress<sup>5</sup>, T.Gress<sup>5</sup>,  
D.Horns<sup>1</sup>, A.Ivanova<sup>5</sup>, S.Kiruhin<sup>5</sup>, E.Konstantinov<sup>5</sup>, E.Korosteleva<sup>3</sup>,  
M.Kunnas<sup>1</sup>, L.Kuzmichev<sup>3,5</sup>, B.Lubsandorzhev<sup>4</sup>, N.Lubsandorzhev<sup>3</sup>,  
R.Mirgazov<sup>5</sup>, R.Mirzoyan<sup>5,7</sup>, R.Monkhoev<sup>5</sup>, R.Nachtigall<sup>1</sup>,  
A.Pakhorukov<sup>5</sup>, V.Platonov<sup>5</sup>, V.Poleschuk<sup>5</sup>, V.Prosin<sup>3</sup>, G.Rubtsov<sup>4</sup>,  
M.Rüger<sup>2,6</sup>, V.Samoliga<sup>5</sup>, A.Saunkin<sup>5</sup>, P.Satunin<sup>4</sup>, D.Spitschan<sup>1</sup>,  
Yu.Semeney<sup>5</sup>, L.Sveshnikova<sup>3</sup>, V.Tabolenko<sup>5</sup>, M.Tluczykont<sup>1</sup>,  
D.Voronin<sup>5</sup>, R.Wischnewski<sup>2</sup>, A.Zagorodnikov<sup>5</sup>, V.Zurbanov<sup>5</sup>

1 : Institute for Experimental physics, University of Hamburg, Luruper Chaussee 149, 22761 Hamburg, Germany

2 : DESY, Platanenallee 6, 15738 Zeuthen, Germany

3 : Skobel'syn institute for Nuclear Physics, Lomonosov Moscow State University, 1 Leninskie gory, 119991 Moscow, Russia

4 : Institute for Nuclear Research of the Russian Academy of Sciences 60th October Anniversary st., 7a, 117312, Moscow, Russia

5 : Institute of Applied Physics ISU, Irkutsk, Russia

6 : Institute for Computer Science, Humboldt-University Berlin, Rudower Chaussee 25, 12489 Berlin, Germany

7 : Max Planck Institut für Physik, Fohringer Ring, München, Germany

E-mail: [andrea.porelli@desy.de](mailto:andrea.porelli@desy.de)

**Abstract.** The Tunka-HiSCORE detector follows the concept of a non-imaging wide-angle EAS Cherenkov array, designed to search for  $\gamma$ -ray sources above 10 TeV and to investigate the spectrum and composition of cosmic-rays above 100 TeV. A prototype array with 9 stations has been deployed in October 2013 at the site of the Tunka experiment in Russia. We describe design and performance of the array data acquisition system DAQ-2, focusing on its timing system based on the White Rabbit technology for sub-nsec time-synchronization over ethernet. First results of EAS arrival direction reconstruction, compared with MC simulations, and tests with artificial light sources verify an excellent performance of the system.

## 1. Introduction

The Tunka-HiSCORE detector is a ground-based air shower Cherenkov array that samples the air shower light front using the non-imaging technique for  $\gamma$ -ray astronomy and cosmic-rays studies [1, 2]. The detector is located in the Tunka Valley, Siberia, at the Tunka-133 array site [3]. Currently, a total area of 0.25 km<sup>2</sup> is instrumented with 28 Tunka-HiSCORE stations. A



hybrid detector system, TAIGA, is under construction, combining as main components a km<sup>2</sup>-scale HiSCORE array with a net of imaging air Cherenkov telescopes [1, 3]. For  $\gamma$ -ray astronomy, the HiSCORE array must achieve a good reconstruction of the air shower arrival direction. For a pointing resolution of  $\sim 0.1^\circ$ , all array stations need to be synchronized with sub-ns time precision [4, 5]. This work presents results from a timing system based on the White Rabbit technology, that was installed in 2012, and operates since 2013/14 with the first Tunka-HiSCORE prototype array. In this paper we use data from dedicated time-calibration runs as well as from normal EAS showers to verify this new technology, which has been used for the first time in a field installation for an astroparticle physics experiment.

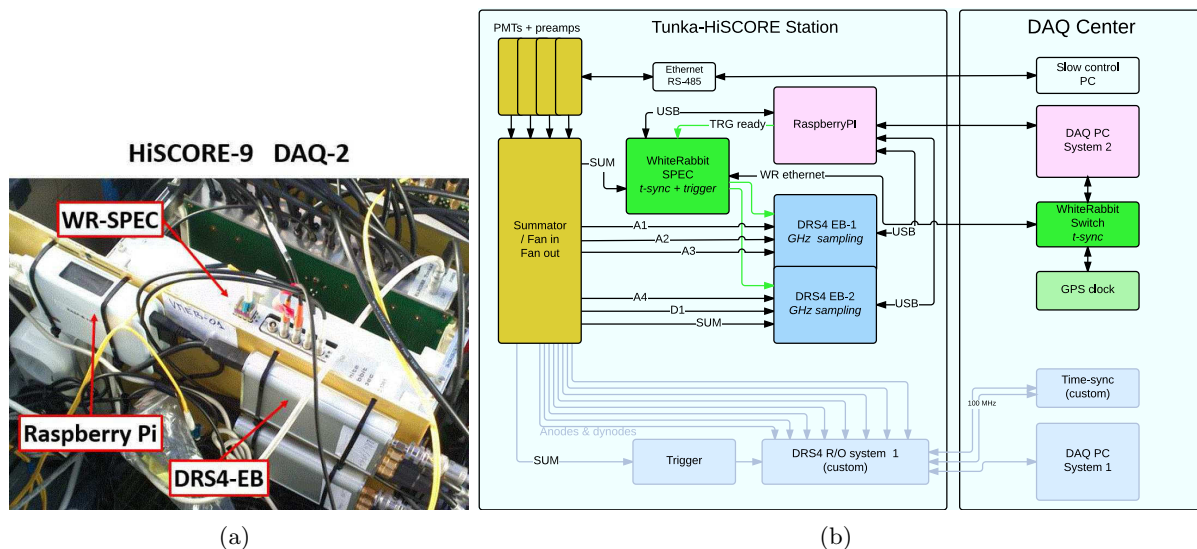


Figure 1: The HiSCORE-9 DAQ-2 system, with DRS4-Evaluation Board and White-Rabbit timing system. (a) Picture of the station setup (with DRS4-EB, WR-SPEC and MiniPC); (b) Schematics of the setup in Station and Center for DAQ-2 (DAQ-1 in grey).

## 2. The HiSCORE-9 array

A first HiSCORE array with 9 stations has been deployed in October 2013, arranged on a regular grid of 3 x 3 stations with 150 m distance and an instrumented area of 0.09 km<sup>2</sup> (HiS-9 array, see section 3 and [1, 3, 6]). Each HiSCORE station is equipped with 4 Photomultiplier Tubes (PMTs) of 8 inch diameter, and with 4 light collectors (Winstone cones), yielding a collection area of 0.50 m<sup>2</sup> and a field of view of 0.6 sr. This first Tunka-HiSCORE array is operated by two independent data acquisition systems (DAQ-1 and DAQ-2), both based on GHz waveform-sampling by the DRS4-chip. Array time-synchronization is done by a custom system in DAQ-1 (with 100MHz clocks sent over separate fibers) and by the ethernet-based White-Rabbit system (WR) in DAQ-2. WR [7] is a new standard for time- and clock-transfer using the extended PTP standard (IEEE 1588) and commercially available basic components; it allows for scalable, flexible and cost-effective sub-nsec synchronization built from large-scale next generation experiments, like CTA, KM3NeT, IceCube-Upgrade [8].

The main purpose of the DAQ-2 system, which is discussed in this paper, is to evaluate this new timing system in a robust DAQ, built from off-the-shelf components. A direct timing performance comparison with DAQ-1 is possible for the 19 new HiSCORE stations installed in October 2014, which combine both systems on a hybrid DAQ-board. Systematic tests of

HiSCORE WR-boards operating since 2012 are given in [9]. Results from the DAQ-1 running since fall 2013 are mentioned in [3].

### 2.1. The HiSCORE-9 DAQ-2 system

DAQ-2 is an autonomous, distributed data taking system, with a central control server that concurrently runs a predefined and exchangable set of tasks per station. It supports remote operation over WAN from multiple locations and incorporates monitoring and self-recovery on hardware error detection. Its main hardware components per station are shown in Fig.1:

- (i) **DRS4 evaluation boards:** to sample PMT pulses at up to 5 GS/s (two boards with 2x4 channels) [10]; for the chosen trace length of 1  $\mu$ s sampling rate is 1 GS/s,
- (ii) **White Rabbit (WR) timing system:** one WR-Node - a SPEC (*Simple PCIe Card*) - per station executes, with custom firmware, the nsec-time stamping and analog pulse triggering [8]. Each SPEC is connected by optical fiber (for synchronization and data transfer) to the main WR-switch in the DAQ center, that provides time synchronization of all the stations and interfaces to a GPS clock. The WR system provides local clocks with a relative phase stability of  $\sim 200$  ps and an absolute clock precision of  $\sim 1$  ns [9],
- (iii) **Raspberry PI:** a mini computer for readout of DRS4 boards, data transfer to the DAQ center and to generate a "readout ready" signal (GPIB) to enable the next SPEC trigger; optionally serves for SPEC monitoring and firmware upgrades.

WR-triggering and time stamping is as follows: The sum of the four PMT anode signals, built by an analog summator board, is sent to a comparator on the WR-SPEC card, which generates a trigger if the signal stays above adjustable threshold for  $t > 9$  ns [9]. Upon a trigger, the WR-clock value is latched with nsec resolution, and sent as trigger time message over the WR-fiber. Synchronous SPEC trigger strobes are sent to both DRS4-EBs, initiating their readout. The intrinsic 1-nsec granularity of the WR-time stamps can be improved, using sub-nsec resolution of anode signals recorded by the DRS4 relative to the WR-strobes. The analysis presented here is based on the WR-time stamps only; with pulse shape analysis an additional improvement is expected.

The eight DRS4 board channels are used to sample four anode signals, their sum, and one dynode as well as the WR strobes (one per DRS4-EB). The trigger thresholds are set to  $\sim 10$  Hz station trigger rates.

### 2.2. Array event building

All HiS-9 stations trigger independently, thus array events are offline selected by requesting coincidence of  $\geq N$  stations within 2  $\mu$ s. Since all WR time-stamps are available in real-time, an array trigger can be easily formed online. This will allow serious data reduction by e.g. station-multiplicity or topology based online array triggers.

## 3. Time calibration

The calibration of the relative arrival times between the stations in a non-imaging Cherenkov detector is critical to achieve precise shower pointing. To investigate the time resolution of the HiS-9 array, a series of calibration runs has been performed - to check single station and full array performance as well as long-term stability.

A bright wide-angle LED light source was positioned outside the array perimeter ( $\sim 200$  m), emitting light pulses with  $\sim 6$  Hz towards all the nine stations. The LED calibration setup is depicted in Fig.2. On top of each station a  $45^\circ$  inclined reflecting screen was added, to redirect

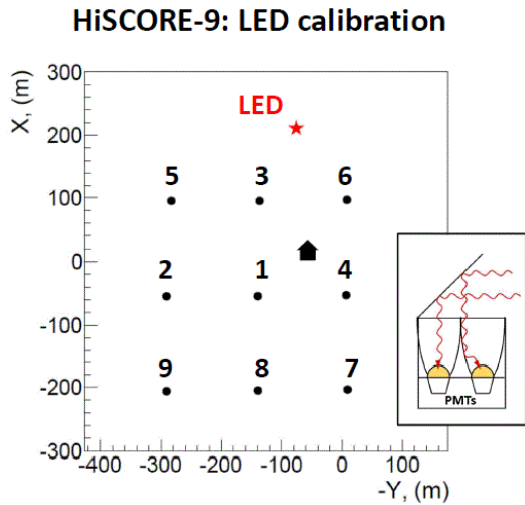


Figure 2: HiS-9 array layout: black house: DAQ center; red star: LED source position during calibration runs; in the small box a scheme of the station setup for the calibration runs.

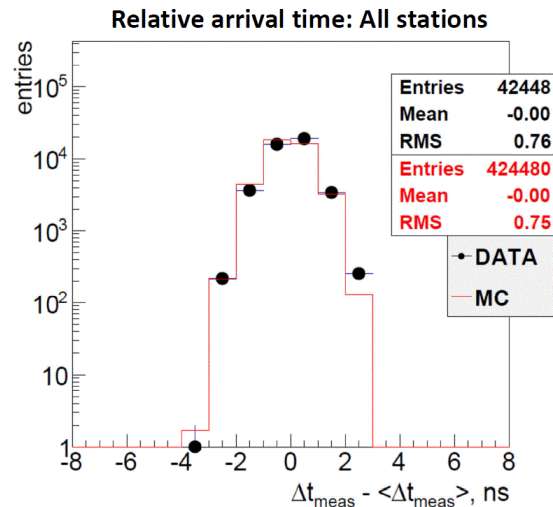


Figure 3: Measured time delay distribution,  $\Delta t_{i3}$  (shifted to zero,  $\Delta t_{i3} - \langle \Delta t_{i3} \rangle$ , to plot all the 9 stations together): dots: Data; red line: simulated events.

the LED light into the stations.

The data sample for this analysis consists of two calibration runs of 15 minutes each, with the second one taken 10 days after the first, from the same position. Only events with all the nine stations triggered are used for the analysis.

### 3.1. Toy Monte-Carlo

We use a toy Monte-Carlo to simulate the response of the array and the measurement system, and to compare to the calibration data. A spherical model is applied for light propagation from the source to the stations; thus the arrival time is given by  $t_i = R_i/c$ , where  $t_i$  is the arrival time of the light to the station  $i$ ,  $R_i$  is the distance between the station and the light source, and  $c$  is the speed of light. To simulate the fluctuation of the timing system (WR), a gaussian time jitter with  $\sigma_{WR}$  is added to the arrival time. The WR time stamps are obtained by rounding the times to 1 ns precision (ns-granularity). We chose  $\sigma_{WR} = 0.45$  ns, as obtained from the raw data analysis, see section 3.2.

### 3.2. Data analysis

The data analysis for the time calibration consists of three steps:

1. Stations time synchronization stability check
2. Determination of the calibration constants  $\Delta t_i^{cal}$
3. Reconstruction of source position coordinates

To check the stability of the time synchronization between the stations, we analyse the raw time differences distributions  $\Delta t_{ij}$  between station  $i$  and a reference station  $j$  (in this case  $j = 3$ , the closest to the LED). The standard deviation of  $\Delta t_{ij}$  is given by (assuming identical stations):

$$\sigma(\Delta t_{ij}) \sim \sqrt{\sigma(t_i)^2 + \sigma(t_j)^2} = \sqrt{2} \cdot \sigma(t_i) \quad (1)$$

$$\sigma(t_i) = \sqrt{(1/\sqrt{12})^2 + \sigma_{WR}^2 + \sigma_X^2} \quad (2)$$

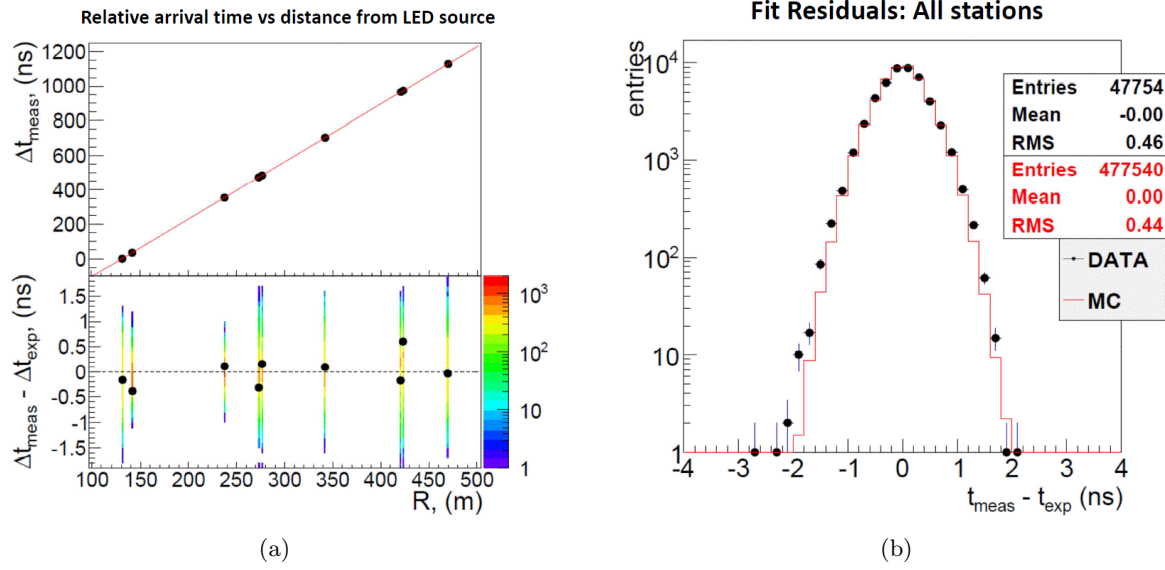


Figure 4: (a) Upper panel: station relative arrival times  $\Delta t_{meas}$  as function of distance  $R$  from the LED light source. The red line gives  $t_i = R_i/c$ . Lower panel: fit residual distributions per station. Black dots show an example of a single triggered event. (b) Distribution of fit residuals (all nine stations superimposed). Black dots: data; Red line: simulated events.

where  $\sigma(t_i)$  is the standard deviation of the measured time at station  $i$ ,  $1/\sqrt{12} = 0.29$  ns is due to the 1 ns time granularity,  $\sigma_{WR}$  is the time jitter of the timing system and  $\sigma_X$  is the time jitter due to apparatus effects (i.e. PMT, electronics, etc.).

From the  $\Delta t_{ij}$ -distribution in Fig.3, we find  $\sigma(t_{ij}) = \sigma(\Delta t_{ij})/\sqrt{2} = 0.54$  ns, which according to eq.2 gives  $\sqrt{\sigma_{WR}^2 + \sigma_X^2} = 0.45$  ns. Thus, we find as an upper limit of the WR-induced time jitter  $\sigma_{WR} \sim 0.45$  ns.

In the second step we compare the distributions of the measured time differences,  $\Delta t_{ij,data}$  with simulation. For each station  $i$ , we calculate the differences between the average values of the two distributions,  $\Delta t_i^{cal} = \overline{\Delta t_{ij,data}} - \overline{\Delta t_{ij,MC}}$ . We consider this  $\Delta t_i^{cal}$  an additional, station-specific time delay w.r.t. the photon arrival time, introduced by station components (analog DAQ components, PMT transient times, cables, WCones, etc.). These values are used as offset calibration constants to correct the arrival time of each station.

The third step of the analysis is the reconstruction of the LED position on an event by event basis, using all nine stations simultaneously. After correcting the arrival times by their calibration constants  $\Delta t_i^{cal}$ , we fit a spherical propagation model for the time  $t_i$  it takes to reach the  $i$ -th station from the source position. An example of a fitted event and the station-wise residual plots is given in Fig.4(a). The standard deviation of the fit residuals, see Fig.4(b), is consistent with the value obtained from the raw data analysis (step 1); and the reconstructed LED coordinates agree with the real ones. This confirms the consistency of the procedure, up to the array level. To summarize, from the LED calibration runs we obtained the station calibration constants  $\Delta t_i^{cal}$ , and derived a conservative upper limit for the HiS-9 WhiteRabbit time jitter of  $\sigma_{WR} \leq 0.45$  ns. An improved estimation of  $\sigma_{WR}$  will be obtained from the DRS4 recorded pulses (for sampling at  $\geq 2$  GS/s), and is expected to reach the  $\sim 0.2$  ns range, as estimated for DAQ-1 [3] and measured in previous WR-field setups [9].

#### 4. EAS shower reconstruction

We reconstruct the first HiS-9 DAQ-2 data, and compare with Monte-Carlo simulations. The selected sample consists of 12 runs for a total of  $\sim 40$  h data taken during clear moonless nights in February/March 2014. Array events are built according to sect.2.2; for this analysis only events with 9 triggered stations are taken into account. A preliminary amplitude calibration is used to convert PMT signals to photo-electrons.

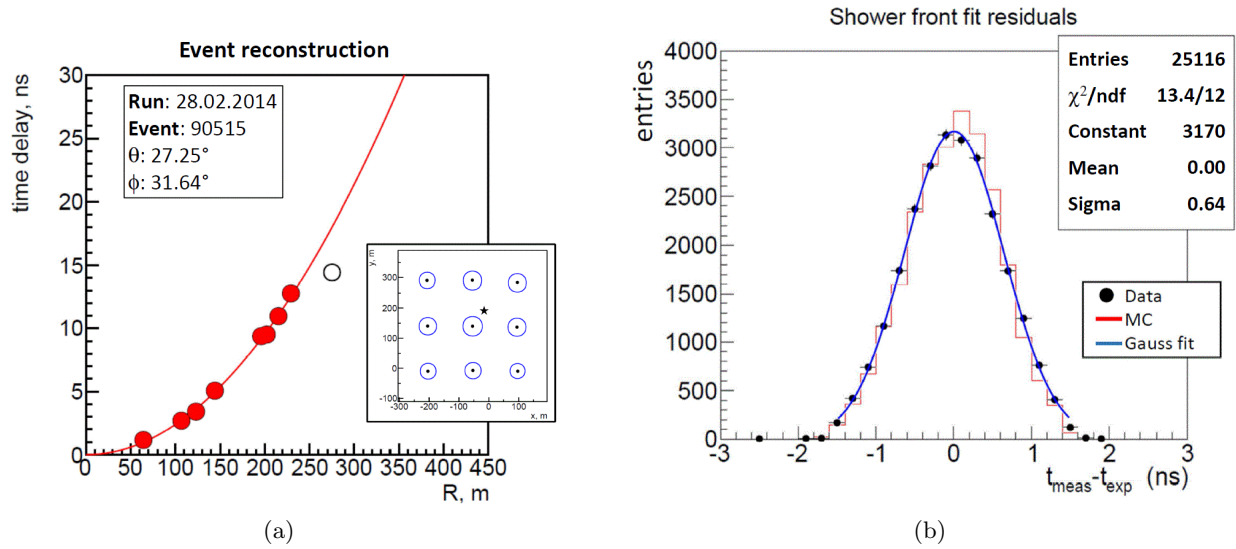


Figure 5: **EAS shower reconstruction.** (a) Arrival time delay vs distance  $R$  from the shower axis. Red/white dots: stations retained / excluded in the final fit; red line: reconstructed shower profile. Small panel: Reconstructed core position (black star), the area of the circles is proportional to  $\log A$ , with  $A$  the station signal amplitude. (b) Distribution of fit residuals after shower reconstruction. Black dots: data; Red line: simulated events; Blue line: gaussian data fit.

##### 4.1. Monte-Carlo simulation

To study the detector response and reconstruction performance, a dedicated Monte-Carlo simulation was done for the HiS-9 array. Air showers have been generated according to the primary proton spectrum ( $dN/dE \propto E^{-2.7}$  and  $10 \leq E \leq 10^3$  TeV) using Corsika v699 [11]; the detector response is simulated with the standard HiSCORE simulation software *sim\_score* [5, 2]. The shower reconstruction is done with *reco\_score*, the HiSCORE reconstruction package [4]. A time jitter with a gaussian distribution of  $\sigma = 0.5$  ns is added to the pulse trigger time, in agreement with the time-resolution results discussed above. All stations are assumed to be identical, which introduces differences between data and Monte-Carlo, in particular for shower core reconstruction.

##### 4.2. Shower reconstruction

The shower reconstruction determines the shower core location ( $x_C, y_C$ ) and the arrival direction (zenith  $\theta$ , azimuth  $\phi$ ). In a first step, an approximate shower direction is obtained by fitting the shower front arrival times with a plane wave. This direction in turn is used for a 2-steps shower-core determination: starting from a first guess for  $x_C$  and  $y_C$  by a center of gravity

method (weighted average of the signal amplitudes recorded in each triggered station), the core position is then obtained by fitting the amplitudes with the amplitude distance function (ADF) using the shower direction, as discussed in [4].

A precision shower direction reconstruction is then obtained by fitting the shower front with an analytical model for the arrival times at each station [12]. The fit is performed recursively, excluding stations with time residuals greater than  $3\sigma$  ( $\sigma = 0.5$  ns, see sect.3); the number of excluded hits is  $\leq 2$  for the  $\sim 92\%$  of the events ( $\leq 1$  for  $\sim 60\%$ ). Figure 5(a) shows an example of a fitted event. The distribution of the fit residuals (Fig.5(b)) follows a gaussian with  $\sigma_{data} = 0.64$  ns, which gives  $\sigma_{WR} \sim 0.57$  ns according to eq.2. We note, that this is close to  $\sigma \sim 0.5$  ns obtained for shower reconstruction in DAQ-1 (which includes a pulse shape analysis). We find stability of the rms from individual stations, over the 10-day run period considered here - showing no time dependence of the WR-synchronization. Figure 6 gives the reconstructed zenith and azimuth distributions, for data and simulated events. We find good agreement between data and MC, given the above mentioned approximations. Small deviations from the MC assumed flat zenith-angular response of the stations sensitivity are currently under investigation.

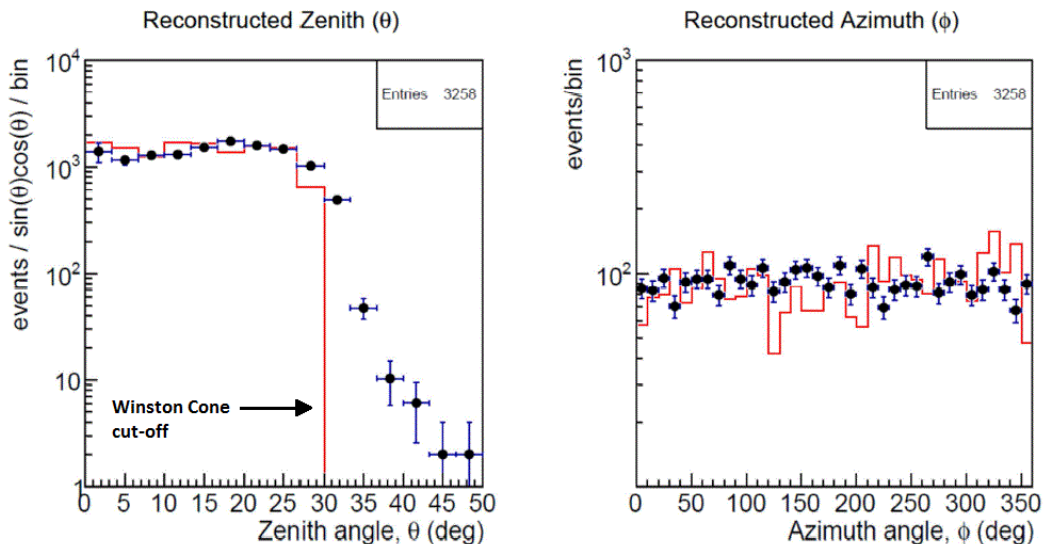


Figure 6: Reconstructed shower direction: Zenith (left), Azimuth (right). Black dots: data events; Red line: simulated events. The cut-off in the reconstructed theta distribution in the Monte-Carlo is due to the used Winston Cone reflection efficiency,  $\epsilon_{WC} = 0$  for  $\theta \geq 28^\circ$ .

## 5. Conclusion

The HiSCORE detector represents a new concept based on the non-imaging Cherenkov technique for cosmic-ray studies and  $\gamma$ -ray astronomy in the PeV energy regime. The HiSCORE-9 array has been operating successfully since October 2013. A dedicated DAQ system based on the WhiteRabbit technology for sub-nsec timing has been taking data. The analysis of LED calibration runs gives an upper limit on the time resolution of the timing system of  $\sigma_t \leq 0.45$  ns, including all experimental effects. This is compatible with standalone laboratory and field results of a 0.2 ns WR-clock jitter.

A first reconstruction of the air showers detected with the HiS-9 array DAQ-2 has been performed. From the shower fit residual distribution we calculate an upper limit on the WR-time resolution of  $\sigma_{WR} \leq 0.57$  ns, consistent with the LED results. From Monte-Carlo studies [4] we

expect for high energies this timing resolution to result in a pointing error of the order of  $0.1^\circ$ . Both the time calibration analysis and shower reconstruction have been performed using only the time information from the WhiteRabbit system, i.e. with 1 ns granularity. An improvement is expected after introducing the corrections due to correct pulse amplitude calibration [6] and PMT pulse shape analysis.

### Acknowledgements

This work was supported by the Russian Federation Ministry of Education and Science (agreements N 14.B25.31.0010, 2014/51, project 1366, zadanie N 3.889.2014/K ), the Russian Foundation for Basic research (grants 13-02-00214, 15-02-10005, 13-02-12095), the Helmholtz Association (Grant HRJRG-303) and the Deutsche Forschungsgemeinschaft (Grant TL51-3).

- [1] M. Tluczykont et al. (TAIGA Collaboration), Towards Gamma-Ray Astronomy with timing array, ECRS-2014, Kiel (Germany), these proceedings
- [2] M. Tluczykont, D. Hampf, D. Horns, D. Spitschan, L. Kuzmichev, V. Prosin, C. Spiering and R. Wischnewski, *Astroparticle Physics* 56 (2014) 4253
- [3] N. Budnev et al. (TAIGA Collaboration), The Tunka experiment: from cosmic ray to gamma astronomy, ECRS-2014, Kiel (Germany), these proceedings
- [4] D. Hampf, M. Tluczykont, D. Horns, *Nuclear Instruments and Methods in Physics Research A* 712 (2013) 137146
- [5] M. Tluczykont, et al., *Advances in Space Research* 48 (2011) 1935.
- [6] S. Epimakhov et al. (Tunka-HiSCORE Collaboration), Amplitude Calibration with the HiSCORE-9 array, ECRS-2014, Kiel (Germany), these proceedings
- [7] J. Serrano et al., The White Rabbit Project, ICALEPCS 2009, [accelconf.web.cern.ch/accelconf/icalepcs2009/papers/tuc004.pdf](http://accelconf.web.cern.ch/accelconf/icalepcs2009/papers/tuc004.pdf)
- [8] M. Brückner and R. Wischnewski, A White Rabbit setup for sub-nsec synchronization, timestamping and time calibration in large scale astroparticle physics experiments, *Proceed. of the 33rd ICRC, 2013, Rio de Janeiro, Brazil, ID-1146*, and White Rabbit in Cosmic Ray Physics and Gamma Astronomy, 8th White Rabbit Workshop, CERN, October 2014, <http://www.ohwr.org/projects/white-rabbit/wiki/Oct2014Meeting>
- [9] M. Brückner et al (Tunka-HiSCORE Collaboration), Results from the WhiteRabbit sub-nsec time synchronization setup at HiSCORE-Tunka, *Proceed. of the 33rd ICRC, 2013, Rio de Janeiro, Brazil, ID-1158*
- [10] Paul Scherrer Institute, Villigen, Switzerland, DRS4 Evaluation Board, <http://www.psi.ch/drs/evaluation-board>.
- [11] K. Bernlöhr, Simulation of Imaging Atmospheric Cherenkov Telescopes with CORSIKA and sim telarray, *Astroparticle Physics* 30 (2008) 149158. [arXiv:0808.2253]
- [12] V. Stamatescu, et al., *Astroparticle Physics* 34 (2011) 886896